RESEARCH ARTICLE

Bone marrow stromal cells interaction with titanium; Effects of composition and surface modification

Murali Krishna Duvvuru[1], Weiguo Han[2], Prantik Roy Chowdhury[1], Sahar Vahabzadeh[1]*, Federico Sciammarella[1], Sherine F. Elsawa[2]*

1 Department of Mechanical Engineering, Northern Illinois University, Dekalb, Illinois, United States of America, **2** Department of Molecular, Cellular and Biomedical Sciences, University of New Hampshire, Durham, New Hampshire, United States of America

* sherine.elsawa@unh.edu (SE); svahabzadeh@niu.edu (SV)

Abstract

Inflammation and implant loosening are major concerns when using titanium implants for hard tissue engineering applications. Surface modification is one of the promising tools to enhance tissue-material integration in metallic implants. Here, we used anodization technique to modify the surface of commercially pure titanium (CP-Ti) and titanium alloy (Ti-6Al-4V) samples. Our results show that electrolyte composition, anodization time and voltage dictated the formation of well-organized nanotubes. Although electrolyte containing HF in water resulted in nanotube formation on Ti, the presence of NH4F and ethylene glycol was necessary for successful nanotube formation on Ti-6Al-4V. Upon examination of the interaction of bone marrow stromal cells (BMSCs) with the modified samples, we found that Ti-6Al-4V without nanotubes induced cell proliferation and cluster of differentiation 40 ligand (CD40L) expression which facilitates B-cell activation to promote early bone healing. However, the expression of glioma associated protein 2 (GLI2), which regulates CD40L, was reduced in Ti-6Al-4V and the presence of nanotubes further reduced its expression. The inflammatory cytokine interleukin-6 (IL-6) expression was reduced by nanotube presence on Ti. These results suggest that Ti-6Al-4V with nanotubes may be suitable implants because they have no effect on BMSC growth and inflammation.

Introduction

Commercially pure titanium (CP-Ti) and titanium alloy (Ti-6Al-4V) are widely used as dental and orthopedic implants due to their biocompatibility, excellent corrosion resistance and desired mechanical properties. This includes properties such as low Young's modulus, low density and fatigue resistance [1–3]. However, the formation of a fibrous capsule around titanium implants and the resultant implant loosening can cause severe pain for patients, which often requires revision surgery [4]. Surface modification techniques such as applying an osteo-conductive coating, alkali treatment, acidic treatment, and electrochemical anodization are promising tools to enhance osseointegration of Ti implants [5]. Among the various techniques,

introducing TiO$_2$ nanotubes on the surface of Ti through anodization has gained attention as it is a simple, cost efficient and well controlled methodology. However, parameters such as electrolyte composition, voltage and the duration of anodization have been shown to alter the morphology of the surface [6,7]. In the current study, we used five different conditions to investigate and compare the effects of substrate composition and anodization parameters on successful formation of nanotubes on both CP-Ti and Ti-6Al-4V [8,9]. We hypothesized that different conditions are needed to achieve well-formed nanotubes on CP-Ti and Ti-6Al-4V.

Several studies reported the efficiency of TiO$_2$ nanotubular layer on *in vitro* cell adhesion and proliferation, protein adsorption, and on *in vivo* osseointegration [10–13]. The presence of nanotubes not only enhances the surface roughness and hydrophilicity, but also activates angiogenic factors [12]. In addition, nanotube incorporation increases *in vivo* collagen and osteocalcin expression, and bone-implant interfacial strength which further improves osseointegration [13]. However, the interaction between nanotubes and bone marrow stromal cells (BMSCs) is less understood and the resultant inflammatory response has not been reported. BMSCs play an important role in blood and stem cell development and differentiation [14,15]. These cells can also differentiate into osteoblasts or adipocytes under the proper cell culture conditions [16], or depending on the type of biomaterial they are cultured on [17]. Therefore, understanding the nature of the interaction between BMSCs and titanium as a function of composition and surface roughness is necessary to predict blood cell development and bone healing.

In this study, we investigated the effects of substrate composition, electrolyte, voltage and anodization time on successful nanotube arrangement and studied the effects of titanium composition and nanotube presence on their interaction with human BMSCs. Nanotube microstructures were evaluated using scanning electron microscopy (SEM) and well-formed structures were used to investigate early proliferation of BMSCs and their inflammatory responses.

Materials and methods

Sample preparation

Grade 2 CP-Ti sheets were purchased from President Titanium, MA, USA. Ti-6Al-4V cylinders were formed using an additive manufacturing technique (LENS) with laser power of 645 W and travel speed of 60 inch/min. These cylinders were then machined and cut into Ti-6Al-4V discs. CP-Ti and Ti-6Al-4V substrates with a diameter of 11 mm and a thickness of 2 mm were grinded using silicon carbide papers from 320 to 800 grit, followed by polishing using a MasterTex polishing cloth. Samples were then cleaned in DI water and acetone, and then air dried. The titanium anode and a platinum foil cathode (Alfa Aesar, Tewksbury, MA,USA) were connected to a DC power supply (Agilent E3612A) and suspended in a beaker containing the electrolyte with different compositions as indicated in Table 1. After anodization, the

Table 1. Anodization process conditions.

Condition	Electrolyte	Voltage (V)	Time (min)
A	1 vol. % HF in DI water	20	45
B	1 vol. % HF in DI water	20	60
C	1 vol. % HF in DI water	30	60
D	1 vol. % HF, 0.5 wt. % NH$_4$F, 10 vol. % DI water in Ethylene Glycol medium	40	60
E	0.25 wt. % NH$_4$F, 2 vol. % DI Water in Ethylene Glycol Medium	30	180

samples were rinsed with DI water and then air dried. The conditions outlined below were selected as previously described [8,9].

Characterization

Surface morphology was evaluated using field emission scanning electron microscope (FESEM; Hitachi S-4500, NY, USA) and elemental analysis was carried out using energy dispersive spectroscopy (EDS, Oxford Instruments, MA, USA). The surface roughness was performed on an 840.6 μm X 840.6 μm area using an optical profiler (Nexview, Zygo Corporation, Middlefield, Connecticut, USA). The contact angle measurements were performed by sessile drop method using a contact angle measurement system (VCA optima, AST Products, Inc., MA, USA). A 2 μl distilled water droplet was used for the test and the contact angle between the droplet and the substrate surface was calculated. The mean and SDs were calculated for both surface roughness and contact angle.

Cell culture

The human bone marrow-derived mesenchymal stromal cell (BMSC) line Saka-T (referred to as Saka cells) was generously provided by Dr. David Roodman (University of Pittsburgh, PA, USA). Cells were cultured in MEM-α supplemented with 10% fetal bovine serum (FBS) and antibiotics/antimycotics (anti-anti) as previously published [18]. Cells were used for experiments when they reached approximately 80–90% confluency.

Proliferation assay, cellular morphology and quantitative reverse-transcription PCR (qRT-PCR)

Cells were seeded at density of $25\text{x}10^3$ and $1\text{x}10^6$ to each Ti disc in triplicate wells in 24-well plate for proliferation assay and qRT-PCR, respectively. Cells were allowed to adhere for approximately 30 minutes and 400 μl of media were carefully added from the side of each well followed by incubation at 37°C. After 3 days, cell culture media was removed and 700 μl of DPBS (Fisher Scientific, Waltham, MA, USA) were used to carefully wash cells without disturbing cells. Ti discs were then placed into a new 24-well plate and 400 μl of DPBS were added to each well followed by 100 μl of XTT working solution (Trevigen, Gaithersburg, MD, USA) was added to each well and incubated at 37°C for 3 hours, followed by data acquisition on an Epoch plate reader (BioTek, Winooski, VT, USA).

For qRT-PCR, $1\text{x}10^6$ cells were used for each Ti disc in triplicate wells in 24-well plate as indicated above. After 24 hours, cell culture media was aspirated, and cells were lysed using 1 ml TRIzol reagent (Life Technologies, Grand Island, NY, USA). Total RNA was isolated following manufacturer's protocol. Reverse transcription reactions were conducted using Moloney murine leukemia virus (M-MLV) reverse transcriptase (Promega, Madison, WI, USA) and qRT-PCR was performed using SYBR Green methodologies a ViiA7 real-time PCR instrument (Life Technologies, Grand Island, NY, USA). To quantify gene expression, GAPDH was used as a housekeeping gene and the following primers were used: GAPDH, 5′-CTCGACTT CAACAGCGACA-3′ (forward) and 5′-GTAGCCAAATTCGTTGTCATACC-3′ (reverse); IL-6, 5′-TCCAAAGATGTAGCCGCCC-3′ (forward) and 5′-CAGTGCCTCTTTGCTGCTTT C-3′ (reverse); GLI2, 5′-CTCCGAGAAGCAAGAAGCCA-3′ (forward) and 5′-GATGCTG CGGCACTCCTT-3′ (reverse), CD40L, 5′-AACATCTGTGTTACAGTGGGCT-3′ (forward) and 5′-AACGGTCAGCTGTTTCCCAT-3′ (reverse); alkaline phosphatase-1 (ALP-1), 5′-CCTACCAGCTCATGCATAACA-3′ (forward) and 5′-GGCTTTCTCGTCACTCTCATA C-3′ (reverse); collagen A-1 (COLA-1), 5′-CGATGGATTCCAGTTCGAGTATG-3′ (forward) and 5′-CGATGGATTCCAGTTCGAGTATG-3′ (reverse); and osteocalcin (OCN),

5'-CAGGCGC TACCTGTATCAAT-3' (forward) and 5'-CGATGTGGTCAGCCAACT-3' (reverse).

Cell morphology was examined using FESEM. After 3 days of culture, samples were removed from culture and fixed with 2% paraformaldehyde/2% glutaraldehyde in 0.1 M phosphate buffer overnight at 4 ˚C. Samples were rinsed with 0.1 M phosphate buffer (three times, followed by fixation with 2% osmium tetroxide (OsO_4) for 2 h at room temperature. Samples were then rinsed again with 0.1 M phosphate buffer three times and dehydrated in ethanol series (30, 50, 70, 95, and 100% (three times for 100% ethanol), followed by dehydration using hexamethyldisilane (HDMS; Fisher Scientific, Waltham, MA, USA).

Statistical analysis

A one-way analysis of variance (ANOVA) was used to analyze data. A p value <0.05 was considered significant. Statistical analysis was performed using GraphPad Prism software (San Diego, CA, USA).

Results

Anodization and sample characterization

Surface morphology of the anodized CP-Ti samples is presented in Fig 1a–1e. Uniform nanotubes with a diameter of ~100 ± 10 nm were generated by using the HF in aqueous electrolyte for 45 min (Fig 1a) and as shown in Fig 1b, increasing the time to 60 min did not affect the morphology. Increasing the voltage to 30 V resulted in formation of random porous structures (Fig 1c). Furthermore, nanotubes with broken structures were formed by having a mixture of NH_4F and HF in as an electrolyte (Fig 1d). Interestingly, as shown in Fig 1e, changing the electrolyte and having NH_4F as the only fluoride ion source in ethylene glycol medium resulted in formation of nanograss-like tubular structures. Nanograss are close-packed clusters of nanotubes on top of nanotubes [9]. Similar anodization parameters were used to investigate the role of time, voltage and electrolyte composition on morphology of samples. As illustrated in Fig 1f and 1g, nanotubes were not completely formed in aqueous electrolytes. While nanotubes had a non-uniform structure at lower voltage and anodization time, a randomly porous structure was obtained by increasing time and voltage (Fig 1h). However, uniform nanotubes on Ti-6Al-4V samples with diameter of ~100 ± 15 nm were achieved using a combination of HF and NH_4F in ethylene glycol (Fig 1i). As shown in Fig 1j, the absence of HF and extended duration time resulted in the formation of nanograss. Taken together, these results indicate that a successful anodization process and uniform nanotube formation depend not only on the anodization parameters, but also on the composition of the Ti substrate.

The optimized anodization conditions that result in well-formed nanotubes on CP-Ti and Ti-6Al-4V were conditions A and D, respectively (referred to as Ti-NT and Ti-6Al-4V -NT, respectively from now on). The surface composition of Ti-NT and Ti-6Al-4V -NT was determined using an EDS detector and the obtained spectrum and elemental analysis are shown in Fig 2. The surface roughness parameters of Ti, Ti-NT, Ti-6Al-4V and Ti-6Al-4V–NT are presented in Table 2 and Fig 3. We found that Ti-NT have a higher surface roughness compared to Ti while no significant change was observed between Ti-6Al-4V and Ti-6Al-4V-NT. Contact angles of samples with water are shown in Fig 4. The contact angles of Ti and Ti-6Al-4V were 44.1˚±4 and 48.9˚±2, respectively. Formation of nanotubes reduced the contact angles to 20.73˚±5 and 14.85˚±5 for Ti-NT and Ti-6Al-4V-NT, respectively which suggests enhanced hydrophilicity after anodization.
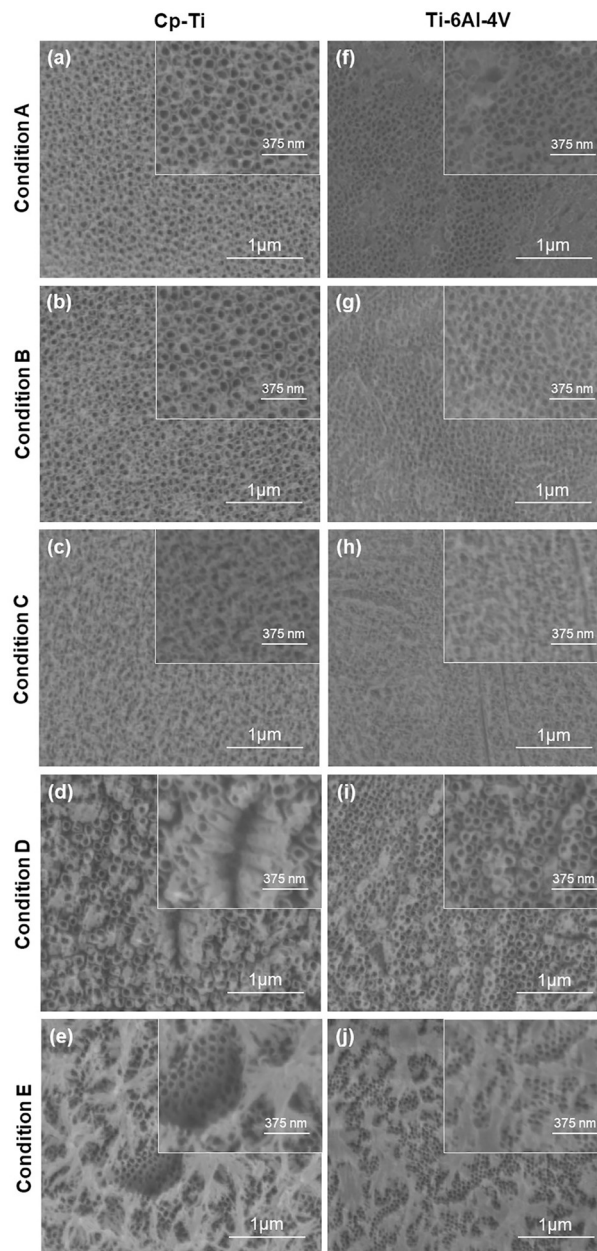
Fig 1. Effect of anodization parameters on surface morphology. Anodization was performed with five different conditions and their effect on nanotubes formation were observed on Cp-Ti (a-e) and Ti-6Al-4V (f-j) using a FESEM. Uniform nanotubes were observed on Ti (a&b) and Ti-6Al-4V (i). Other anodization conditions resulted in nonuniform distribution and/or distortion in structure of nanotubes (c, d, f, g, h) and formation of nanograss (e and j).

https://doi.org/10.1371/journal.pone.0216087.g001

Adhesion of bone marrow stromal cells (BMSCs) on Ti substrates

The effects of Ti substrate composition and the presence of nanotubes on BMSC attachment and cellular morphology after 3 days of culture were investigated by SEM and the results are shown in Fig 5A. Regardless of composition and surface morphology, BMSCs attached to Ti and Ti-6Al-4V samples and demonstrated well-spread morphologies. We also investigated BMSC adhesion to Ti substrates at earlier times (6 hours following seeding) and assed cell
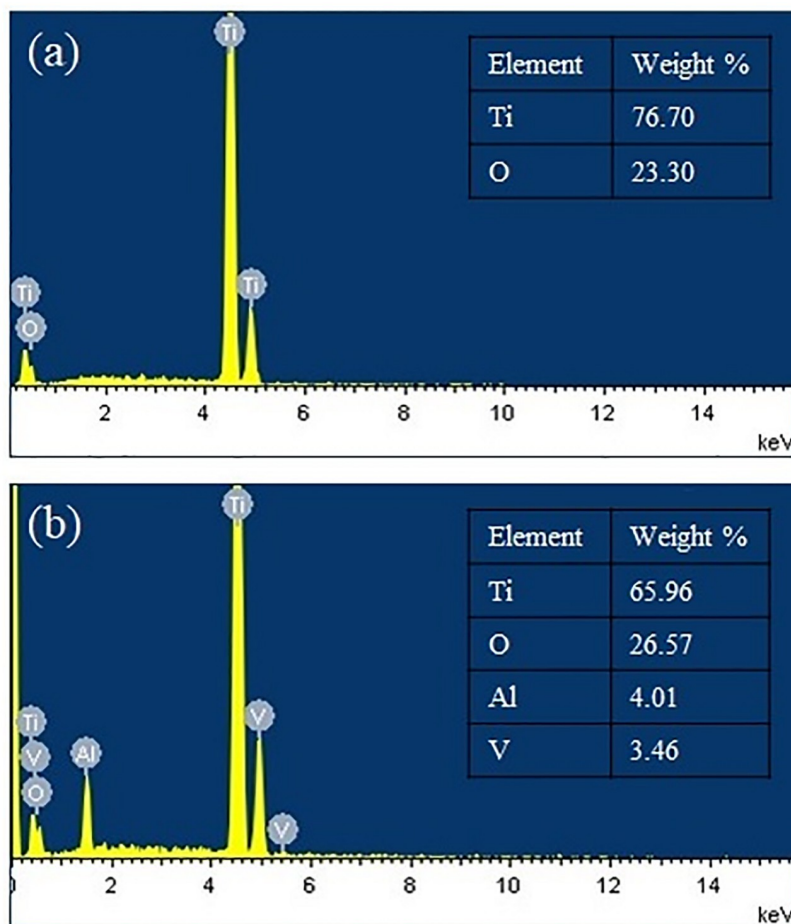
Fig 2. Elemental analysis of Ti substrates. The EDS elemental analysis of (a) Ti-NT and (b) Ti-6Al-4V-NT showing presence of only Ti and O in Ti-NT, while Ti, Al, V and O are found in Ti-6Al-4V.

https://doi.org/10.1371/journal.pone.0216087.g002

adhesion by XTT assay. We found no differences in cell adhesion between the different substrates compared to adhesion of BMSCs on CP-Ti (p = 0.6056)(Fig 5B).

Assessment of cell growth, differentiation and inflammatory gene expression on Ti substrates

The effect of composition and surface treatment on cell proliferation was investigated using XTT assay and results are presented in Fig 6. As compared to Ti, BMSC proliferation was significantly higher on Ti-6Al-4V (p = 0.0203). However, the incorporation of nanotubes to Ti-

Table 2. Surface roughness parameters of the Ti substrates.

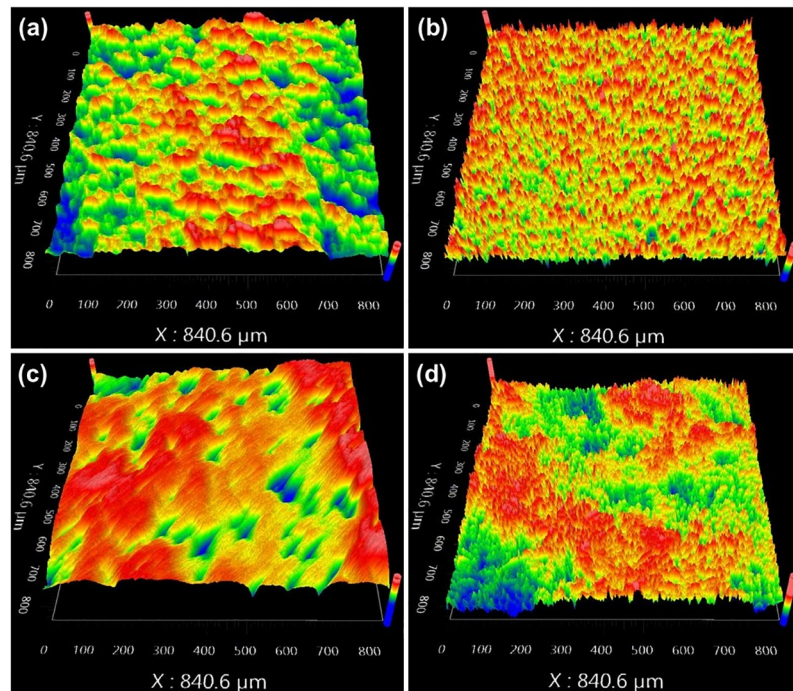| Sample	Sa (nm)	Sq (nm)	Sz (nm)
Ti	32±2	39.75±2	342.25±87
Ti-NT	196±18	255.9±28	2605.25±113
Ti-6Al-4V	36.25±2	46.5±3	419±72
Ti-6Al-4V-NT	40.25±6	50.5±8	633±83

https://doi.org/10.1371/journal.pone.0216087.t002

Fig 3. Surface roughness of Ti substrates. Surface roughness of the Ti substrates (a) Ti (b) Ti-NT (c) Ti-6Al-4V (d) Ti-6Al-4V-NT, was determined by an optical profiler. Shows increase in roughness of samples after anodization.
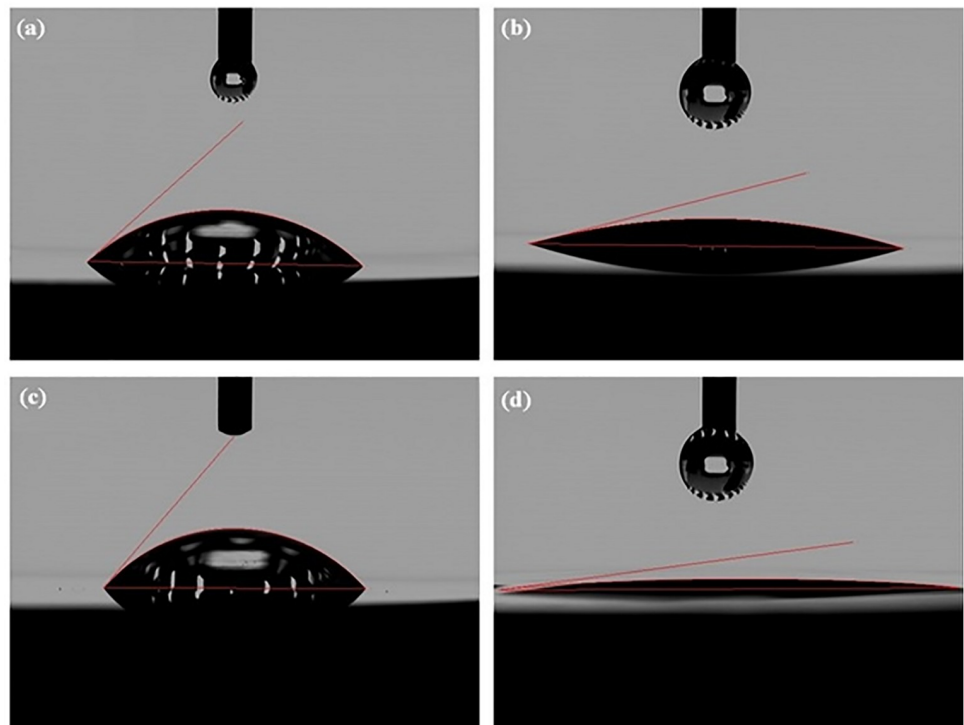
Fig 4. Anodization increases hydrophilicity. Contact angle of (a) Ti (b) Ti-NT (c) Ti-6Al-4V (d) Ti-6Al-4V-NT. Contact angles in anodized samples (b and d) are significantly less that untreated samples showing the effective role of anodization on increasing hydrophilicity.
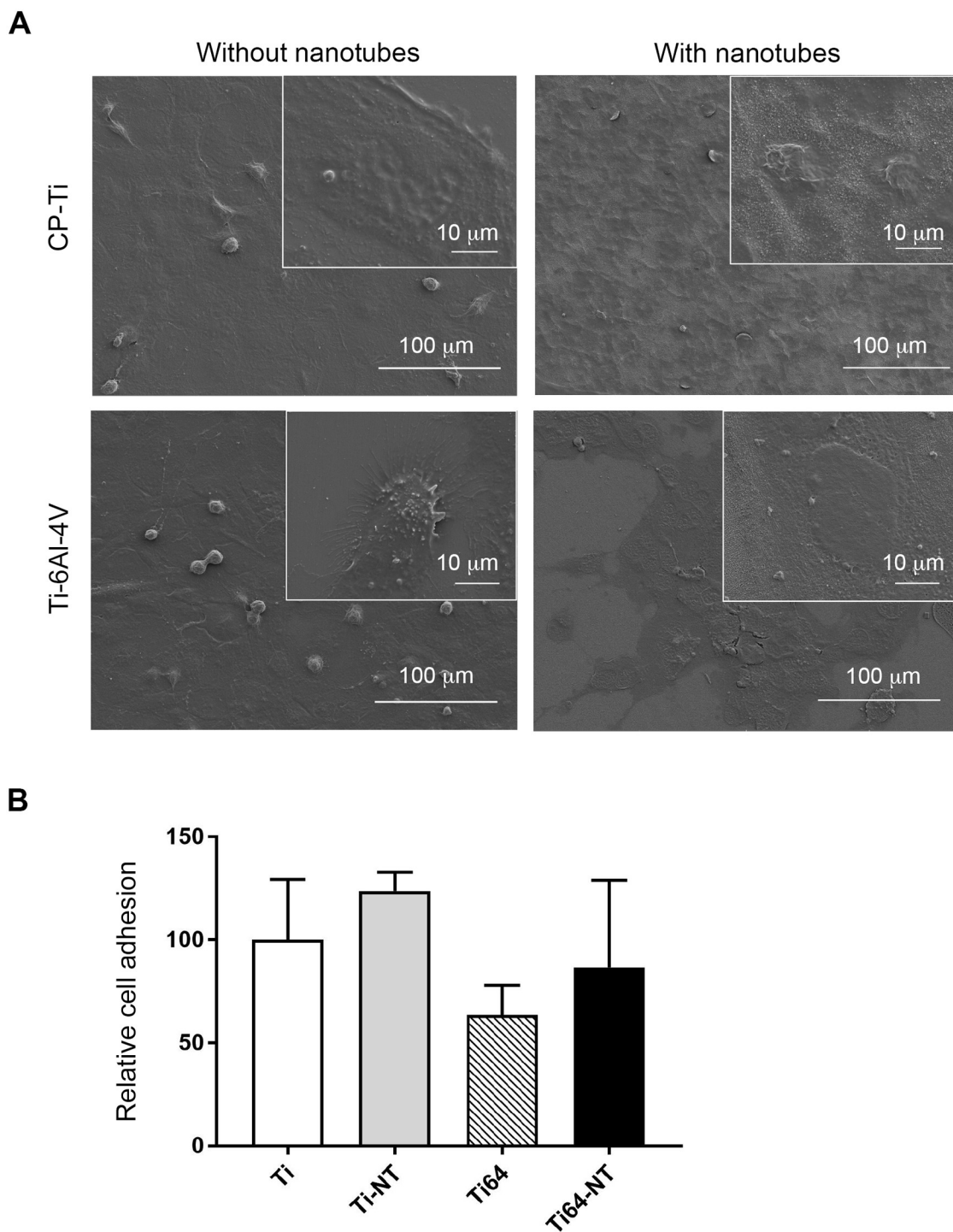
A

B

Fig 5. Cellular morphology on Ti substrates. a) Saka cells were grown on Ti discs as indicated in materials and methods followed by examination of cellular morphology using FESEM. b) Saka cells were allowed to adhere to Ti discs for 6 hours followed by investigation of cell adhesion by XTT assay.
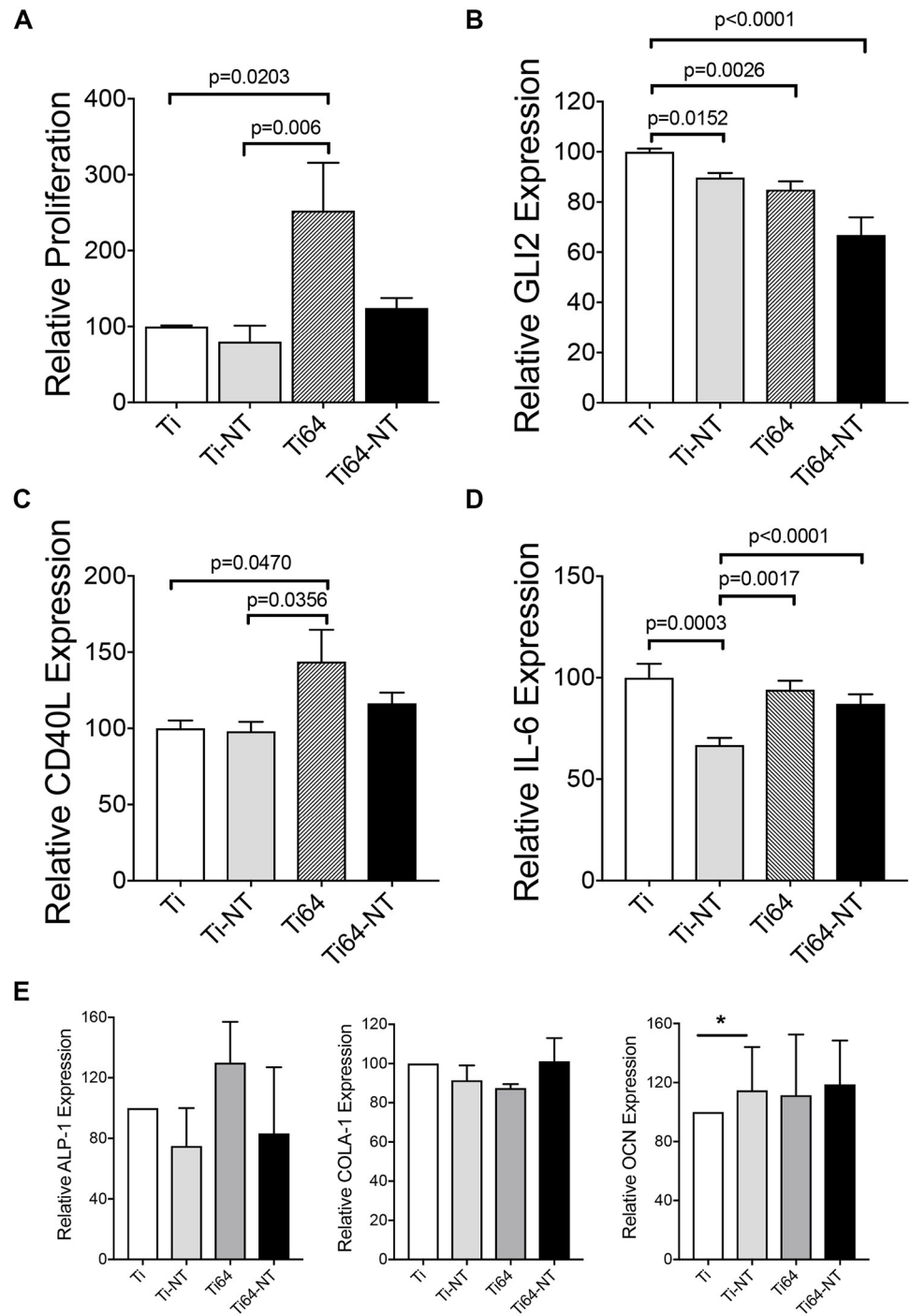
https://doi.org/10.1371/journal.pone.0216087.g005

Fig 6. Effect of composition and surface morphology on growth of BMSCs and inflammation. a) Saka cells were allowed to adhere on material as indicated in methods for 3 days followed by XTT assay to determine cell proliferation. qRT-PCR for the inflammatory markers b) GLI2, c) CD40L and d) IL-6. E) Saka cells were allowed to adhere A similar experiment was performed to determine the expression of differentiation markers alkaline phosphatase 1 (ALP-1), Collagen A-1 (COLA-1) and osteocalcin (OCN) on the different substrates by qRT-PCR. Data are presented as averages of 2 independent experiments, each performed in triplicate and the bars represent means ± SEM.

https://doi.org/10.1371/journal.pone.0216087.g006

6Al-4V (Ti-6Al-4V -NT) reduced the proliferation of BMSC compared with Ti-6Al-4V, suggesting that the incorporation of nanotubes may provide therapeutic efficacy by promoting bone formation [19] but not BMSC growth. We have previously reported that the glioma-associated protein 2 (GLI2) is expressed by BMSCs and modulates inflammatory genes [18,20,21]. Therefore, we examined the expression of GLI2 in BMSCs grown on Ti and Ti-6Al-4V in the presence or absence of nanotubes. We found a decrease in GLI2 expression by BMSCs grown on Ti-NT compared with CP-Ti (Fig 6b) suggesting that downstream inflammatory genes may be reduced. Although Ti-6Al-4V induced BMSC growth, it resulted in a reduction in GLI2 expression (Fig 6b). Furthermore, Ti-6Al-4V-NT had significantly lower GLI2 expression compared with Ti alone. We have previously reported that GLI2 can regulate the expression of CD40 ligand (CD40L) in BMSCs [18]. CD40L expression was increased in BMSCs grown on Ti-6Al-4V but not Ti-6Al-4V -NT (Fig 6c). This pattern of CD40L expression is consistent with the pattern of cell proliferation shown in Fig 6a. We further examined the expression of the pleiotropic cytokine interleukin-6 (IL-6), which is regulated, in part, by GLI2 [20]. Although Ti-6Al-4V induced BMSC proliferation, this did not increase IL-6 expression (Fig 6d). Additionally, Ti-NT, but not Ti-6Al-4V-NT, reduced IL-6 expression. Taken together, these results suggest that the incorporation of NT on Ti-6Al-4V may be therapeutically beneficial by promoting osteoblast attachment as previously reported [22], without inducing BMSC growth, while not altering the inflammatory response required to facilitate healing. Interestingly, BMSCs cultured on CP-Ti and Ti-6Al-4V did not express osteoblast differentiation markers alkaline phosphatase-1 (ALP-1), collagen A-1 (COLA-1) or osteocalcin (OCN) suggesting that the different Ti substrates and the presence of nanotubes did not affect BMSC differentiation (Fig 6e).

Discussion

TiO$_2$ nanotubes are of great interest due to their excellent physical, mechanical and biological properties. Previous studies have reported that nanotubes enhance the protein adsorption and osteoblast cell attachment which improves bioactivity [23,24]. In this study, we fabricated nanotubes on the surface of both CP-Ti and Ti-6Al-4V using experimental different conditions. These conditions were selected based on previous work for different types of titanium alloys [8,9]. We found that formation of nanotubes depends on both anodization parameters and substrate composition. This is in line with the literature where formation of nanotubes was confirmed on IMI834 titanium alloy using H$_3$PO$_4$+HF electrolyte, whereas no nanotube was found on CP-Ti and Ti-6Al-4V substrates using the same anodization conditions, showing the dependency of the successful anodization on phase composition of Ti and its alloys [6]. Nanotubes formed by anodization are usually referred to as TiO$_2$ nanotubes. However, pure TiO$_2$ nanotubes are formed only on CP-Ti while the presence of Al and V in Ti-6Al-4V results in formation of Ti-Al-V-O nanotubes. High amounts of Al decrease the dissolution rate, while the presence of V increases the dissolution rate which affect nanotube formation [25]. Similar to Al and V, increase in Zr content in Ti-alloy increases interspace between TiO$_2$ nanotubes [26]. However, regardless of Ti composition, the presence of fluoride ions appears crucial for the growth of TiO$_2$ nanotubes, as F$^-$ helps in the chemical dissolution of the oxide layer. In addition to F$^-$, water content and the viscosity of ethylene glycol (EG) alter nanotube formation as they alter the rate of oxidation and diffusion of ions in the electrolyte, respectively [27,28].

The EDS results confirm the presence of oxygen on both Ti-NT and Ti-6Al-4V -NT which was 23.30 and 26.57 wt% respectively while no fluorine was detected (Fig 2). They also confirm the presence of Al and V on Ti-6Al-4V -NT with a percentage of 4.01% and 3.46% respectively

(Fig 2). Surface roughness and wettability are the most important factors that influence cell attachment [29,30]. It was reported that the presence nanotubes increases the surface roughness which further improves osseointegration [31]. Our results (Fig 3) are in agreement with the studies with one exception. The presence of nanotubes on Ti increased the surface roughness while no significant change was observed in surface roughness of Ti-6Al-4V with and without nanotubes (Fig 3). This might be due to the presence of porosity in LENS processed Ti-6Al-4V. On the other hand, the results of wettability are in line with the studies reporting the presence of nanotubes reduces the contact angle and increases the hydrophilicity of the surface [32]. Both Ti-NT and Ti-6Al-4V-NT showed improved surface hydrophilicity (Fig 4). Highly hydrophilic surfaces increase cell attachment and improve bioactivity due to enhanced interaction between cells and material [33–35].

We report that in the presence of nanotubes, BMSCs showed well-spread cellular morphology (Fig 5) which may be related to enhanced hydrophilicity in the presence of nanotubes [12]. In addition to morphology, SEM images show the ability of BMSCs to attach and spread on both CP-Ti and Ti-6Al-4V in the presence and absence of nanotubes (Fig 5). Our results also show that the presence of nanotubes reduced proliferation of BMSC which suggests that nanotubes may provide therapeutic efficacy by promoting bone formation as described in earlier *in vivo* studies [19] but not BMSC growth or their differentiation into osteoblasts (Fig 6). Furthermore, when we investigated inflammatory gene expression, we found a reduction in GLI2 expression with Ti-NT and Ti-6Al-4V-NT compared to Ti and Ti-6Al-4V suggesting that downstream inflammatory genes that are regulated by this protein may also be reduced. We previously showed that GLI2 can regulate the expression of CD40 ligand (CD40L) in BMSCs [18]. CD40L is a protein that is expressed on the surface of various cells including stromal cells [18] and plays a role in B-cell activation. Recruitment of B-cells and other immune cells has been shown to promote early bone healing [36]. These results suggest that formation of well-organized nanotubes depend on titanium composition and anodization parameters and Ti-6Al-4V -NT may provide a benefit by maintaining IL-6 expression to allow an initial inflammatory response to mediate healing while not inducing prolonged activation of other immune cells.

Conclusion

In this study, we investigated the effects of substrate composition, electrolyte, voltage and anodization time on successful nanotube arrangement on Ti substrate and found both substrate composition and anodization parameters effect the formation of nanotubes. We also studied the effects of titanium composition and nanotube presence on their interaction with human BMSCs. For bone tissue engineering applications, the incorporation of NT on Ti-6Al-4V may be therapeutically beneficial due to the ease of manufacturing. Furthermore, this will promote osteoblast attachment [22], without inducing BMSC growth, or altering the inflammatory response required to facilitate healing.

Supporting information

S1 Table. Surface roughness and contact angle measurements. Raw data for measurements of surface roughness and contact angles.
(PDF)

S2 Table. XTT assay for Figs 6A and 5B. Raw data from experiments of relative cell proliferation.
(PDF)

S3 Table. Gene expression for Fig 6B–6D. Raw data from experiments to determine relative gene expression.
(PDF)

S4 Table. Cell differentiation Fig 6E. Raw data from experiments to determine cell differentiation markers by qRT-PCR.
(PDF)

Acknowledgments

Author Contributions

Conceptualization: Sahar Vahabzadeh, Sherine F. Elsawa.

Data curation: Prantik Roy Chowdhury.

Investigation: Murali Krishna Duvvuru, Weiguo Han, Federico Sciammarella.

Project administration: Sahar Vahabzadeh, Sherine F. Elsawa.

Resources: Sahar Vahabzadeh, Sherine F. Elsawa.

Supervision: Sahar Vahabzadeh, Sherine F. Elsawa.

Writing – original draft: Murali Krishna Duvvuru, Weiguo Han, Sahar Vahabzadeh, Federico Sciammarella, Sherine F. Elsawa.

References

1. Schiff N, Grosgogeat B, Lissac M, Dalard F. Influence of fluoride content and pH on the corrosion resistance of titanium and its alloys. Biomaterials. 2002; 23: 1995–2002. PMID: 11996041

2. Geetha M, Singh AK, Asokamani R, Gogia AK. Ti based biomaterials, the ultimate choice for orthopaedic implants–A review. Prog Mater Sci. 2009; 54: 397–425. https://doi.org/10.1016/j.pmatsci.2008.06.004

3. Bortolan C, Campanelli L, Bolfarini C, Oliveira N. Fatigue strength of Ti-6A1-4V alloy with surface modified by TiO2 nanotubes formation. Mater Lett. 2016; 177: 46–49. https://doi.org/10.1016/j.matlet.2016.04.188

4. Suska F, Emanuelsson L, Johansson A, Tengvall P, Thomsen P. Fibrous capsule formation around titanium and copper. J Biomed Mater Res A. 2008; 85: 888–896. https://doi.org/10.1002/jbm.a.31575 PMID: 17896778

5. Liu X, Chu PK, Ding C. Surface modification of titanium, titanium alloys, and related materials for biomedical applications. Mater Sci Eng R Rep. 2004; 47: 49–121. https://doi.org/10.1016/j.mser.2004.11.001

6. Yashwanth IVS, Gurrappa I. The effect of titanium alloy composition in synthesis of Titania nanotubes. Mater Lett. 2015; 142: 328–331. https://doi.org/10.1016/j.matlet.2014.12.010

7. Luo B, Yang H, Liu S, Fu W, Sun P, Yuan M, et al. Fabrication and characterization of self-organized mixed oxide nanotube arrays by electrochemical anodization of Ti–6Al–4V alloy. Mater Lett. 2008; 62: 4512–4515. https://doi.org/10.1016/j.matlet.2008.08.015

8. Shivaram A, Bose S, Bandyopadhyay A. Thermal degradation of TiO2 nanotubes on titanium. Appl Surf Sci. 2014; 317: 573–580. https://doi.org/10.1016/j.apsusc.2014.08.107

9. Wang J, Li H, Sun Y, Bai B, Zhang Y, Fan Y. Anodization of Highly Ordered TiO2 Nanotube Arrays Using Orthogonal Design and Its Wettability. Int J Electrochem Sci. 2016; 11: 15.

10. Das K, Bose S, Bandyopadhyay A. TiO2 nanotubes on Ti: Influence of nanoscale morphology on bone cell–materials interaction. J Biomed Mater Res A. 2009; 90A: 225–237. https://doi.org/10.1002/jbm.a.32088 PMID: 18496867

11. Yao C, Slamovich EB, Webster TJ. Enhanced osteoblast functions on anodized titanium with nanotube-like structures. J Biomed Mater Res A. 2008; 85A: 157–166. https://doi.org/10.1002/jbm.a.31551 PMID: 17688267

12. Beltrán-Partida E, Valdéz-Salas B, Moreno-Ulloa A, Escamilla A, Curiel MA, Rosales-Ibáñez R, et al. Improved in vitro angiogenic behavior on anodized titanium dioxide nanotubes. J Nanobiotechnology. 2017; 15. https://doi.org/10.1186/s12951-017-0247-8 PMID: 28143540

13. Xia L, Feng B, Wang P, Ding S, Liu Z, Zhou J, et al. In vitro and in vivo studies of surface-structured implants for bone formation. Int J Nanomedicine. 2012; 7: 4873–4881. https://doi.org/10.2147/IJN.S29496 PMID: 23028216

14. Krebsbach PH, Kuznetsov SA, Bianco P, Gehron Robey P. Bone Marrow Stromal Cells: Characterization and Clinical Application. Crit Rev Oral Biol Med. 1999; 10: 165–181. https://doi.org/10.1177/10454411990100020401 PMID: 10759420

15. Abbuehl J-P, Tatarova Z, Held W, Huelsken J. Long-Term Engraftment of Primary Bone Marrow Stromal Cells Repairs Niche Damage and Improves Hematopoietic Stem Cell Transplantation. Cell Stem Cell. 2017; 21: 241–255.e6. https://doi.org/10.1016/j.stem.2017.07.004 PMID: 28777945

16. Pozio A, Palmieri A, Girardi A, Cura F, Carinci F. Titanium nanotubes stimulate osteoblast differentiation of stem cells from pulp and adipose tissue. Dent Res J. 2012; 9: S169–S174. https://doi.org/10.4103/1735-3327.109745 PMID: 23814578

17. Deligianni DD. Multiwalled carbon nanotubes enhance human bone marrow mesenchymal stem cells' spreading but delay their proliferation in the direction of differentiation acceleration. Cell Adhes Migr. 2014; 8: 558–562. https://doi.org/10.4161/cam.32124 PMID: 25482646

18. Han W, Jackson DA, Matissek SJ, Misurelli JA, Neil MS, Sklavanitis B, et al. Novel Molecular Mechanism of Regulation of CD40 Ligand by the Transcription Factor GLI2. J Immunol Baltim Md 1950. 2017; 198: 4481–4489. https://doi.org/10.4049/jimmunol.1601490 PMID: 28461568

19. Bandyopadhyay A, Shivaram A, Tarafder S, Sahasrabudhe H, Banerjee D, Bose S. In vivo response of laser processed porous titanium implants for load-bearing implants. Ann Biomed Eng. 2017; 45: 249–260. https://doi.org/10.1007/s10439-016-1673-8 PMID: 27307009

20. Elsawa SF, Almada LL, Ziesmer SC, Novak AJ, Witzig TE, Ansell SM, et al. GLI2 transcription factor mediates cytokine cross-talk in the tumor microenvironment. J Biol Chem. 2011; 286: 21524–21534. https://doi.org/10.1074/jbc.M111.234146 PMID: 21454528

21. Jackson DA, Smith TD, Amarsaikhan N, Han W, Neil MS, Boi SK, et al. Modulation of the IL-6 Receptor α Underlies GLI2-Mediated Regulation of Ig Secretion in Waldenström Macroglobulinemia Cells. J Immunol Baltim Md 1950. 2015; 195: 2908–2916. https://doi.org/10.4049/jimmunol.1402974 PMID: 26238488

22. Ku C-H, Pioletti DP, Browne M, Gregson PJ. Effect of different Ti-6Al-4V surface treatments on osteoblasts behaviour. Biomaterials. 2002; 23: 1447–1454. PMID: 11829440

23. El-wassefy NA, Hammouda IM, Habib ANEA, El-awady GY, Marzook HA. Assessment of anodized titanium implants bioactivity. Clin Oral Implants Res. 2014; 25: e1–9. https://doi.org/10.1111/clr.12031 PMID: 23173838

24. Lu R, Wang C, Wang X, Wang Y, Wang N, Chou J, et al. Effects of hydrogenated TiO2 nanotube arrays on protein adsorption and compatibility with osteoblast-like cells. Int J Nanomedicine. 2018; 13: 2037–2049. https://doi.org/10.2147/IJN.S155532 PMID: 29670348

25. Li Y, Ding D, Ning C, Bai S, Huang L, Li M, et al. Thermal stability and in vitro bioactivity of Ti-Al-V-O nanostructures fabricated on Ti6Al4V alloy. Nanotechnology. 2009; 20: 065708. https://doi.org/10.1088/0957-4484/20/6/065708 PMID: 19417402

26. Kim W-G, Choe H-C, Ko Y-M, Brantley WA. Nanotube morphology changes for Ti–Zr alloys as Zr content increases. Thin Solid Films. 2009; 517: 5033–5037. https://doi.org/10.1016/j.tsf.2009.03.165

27. Lee B-G, Choi J-W, Lee S-E, Jeong Y-S, Oh H-J, Chi C-S. Formation behavior of anodic TiO2 nanotubes in fluoride containing electrolytes. Trans Nonferrous Met Soc China. 2009; 19: 842–845. https://doi.org/10.1016/S1003-6326(08)60361-1

28. Grimes CA, Mor GK. TiO2 Nanotube Arrays: Synthesis, Properties, and Applications. Springer Science & Business Media; 2009.

29. Oh S, Jin S. Titanium oxide nanotubes with controlled morphology for enhanced bone growth. Mater Sci Eng C. 2006; 26: 1301–1306. https://doi.org/10.1016/j.msec.2005.08.014

30. Ercan B, Taylor E, Alpaslan E, Webster TJ. Diameter of titanium nanotubes influences anti-bacterial efficacy. Nanotechnology. 2011; 22: 295102. https://doi.org/10.1088/0957-4484/22/29/295102 PMID: 21673387

31. Zareidoost A, Yousefpour M, Ghaseme B, Amanzadeh A. The relationship of surface roughness and cell response of chemical surface modification of titanium. J Mater Sci Mater Med. 2012; 23: 1479–1488. https://doi.org/10.1007/s10856-012-4611-9 PMID: 22460230

32. Shin DH, Shokuhfar T, Choi CK, Lee S-H, Friedrich C. Wettability changes of TiO 2 nanotube surfaces. Nanotechnology. 2011; 22: 315704. https://doi.org/10.1088/0957-4484/22/31/315704 PMID: 21727317

33. Brammer KS, Oh S, Cobb CJ, Bjursten LM, van der Heyde H, Jin S. Improved bone-forming functionality on diameter-controlled TiO2 nanotube surface. Acta Biomater. 2009; 5: 3215–3223. https://doi.org/10.1016/j.actbio.2009.05.008 PMID: 19447210

34. Li BE, Li Y, Min Y, Hao JZ, Liang CY, Li HP, et al. Synergistic effects of hierarchical hybrid micro/nano-structures on the biological properties of titanium orthopaedic implants. RSC Adv. 2015; 5: 49552–49558. https://doi.org/10.1039/C5RA05821J

35. Indira K, Mudali UK, Rajendran N. In-vitro biocompatibility and corrosion resistance of strontium incorporated TiO2 nanotube arrays for orthopaedic applications. J Biomater Appl. 2014; 29: 113–129. https://doi.org/10.1177/0885328213516821 PMID: 24346137

36. Könnecke I, Serra A, Khassawna TE, Schlundt C, Schell H, Hauser A, et al. T and B cells participate in bone repair by infiltrating the fracture callus in a two-wave fashion. Bone. 2014; 64: 155–165. https://doi.org/10.1016/j.bone.2014.03.052 PMID: 24721700